

## Weak $K$ hindrance manifested in $\alpha$ decay of the $^{178}\text{Hf}^{m2}$ isomer

S. A. Karamian,<sup>1</sup> J. J. Carroll,<sup>2</sup> S. Iliev,<sup>1</sup> and S. P. Tretyakova<sup>1</sup>

<sup>1</sup>*Flerov Laboratory of Nuclear Reactions, Joint Institute for Nuclear Research, Dubna, RU-141980, Russia*

<sup>2</sup>*Department of Physics and Astronomy, Youngstown State University, Youngstown, Ohio 44555, USA*

(Received 18 July 2006; published 10 May 2007)

An experiment has been performed to detect the  $\alpha$  emission mode in  $^{178}\text{Hf}^{m2}$  isomer decay and a partial half-life of  $(2.5 \pm 0.5) \times 10^{10}$  y was measured. It was concluded that  $\alpha$  decay is strongly retarded by the centrifugal barrier arising due to the high spin of this isomeric state. Additional analysis shows, however, that the  $K$ -hindrance in this  $\alpha$  decay is relatively weak, despite the strong manifestation of spin-hindrance.

DOI: [10.1103/PhysRevC.75.057301](https://doi.org/10.1103/PhysRevC.75.057301)

PACS number(s): 23.60.+e, 21.10.Tg, 27.70.+q

Electromagnetic decay of the noted 31-year-lived isomer  $^{178}\text{Hf}^{m2}$  has been studied extensively (see Ref. [1] and references therein). The level structure of this isotope was also examined using spectroscopic techniques in many reaction studies, such as those of Refs. [2,3]. Until now, however,  $\alpha$  decay of this isomer has not been observed.

A scheme of the process according to the tabulated data of Refs. [4,5] is given in Fig. 1. A maximum energy release in the  $\alpha$  decay corresponds to the transition from the isomeric level to the ground state in the daughter  $^{174}\text{Yb}$  nucleus. The value of  $Q_\alpha = 4.53$  MeV allows  $\alpha$  decay with a half-life on the order of days, much shorter than that due to electromagnetic decay. However, the isomer-to-ground state  $\alpha$  decay spans a 16-unit change in angular momentum and should be strongly suppressed by the centrifugal barrier. Additional structure hindrance may arise due to the  $K$  quantum number as  $\Delta K = 16$  for this transition. The total  $Q_\alpha$  for decay of the ground and first isomeric ( $m1$ ) states of  $^{178}\text{Hf}$  are relatively low and should correspond to very long  $\alpha$  decay half-lives according to the known systematics.

For mid- $Z$  elements, alpha decay is typically observed for short-lived neutron-deficient isotopes. Considering elements ranging from Nd to Pb and isotopes thereof bounded by the magic numbers  $N > 82$  and  $Z \leq 82$ ,  $\alpha$  decay energies  $E_\alpha$  to specific daughter states are known. In many cases the corresponding partial  $\alpha$  decay half-lives have been measured [5]. The hafnium isotopes lie in the center of this range of nuclides, having well-deformed axially symmetric prolate shapes, and it can be expected that they should obey the semi-empirical systematics.

A Geiger-Nuttall plot [6] is shown in Fig. 2 for even- $Z$  nuclei, evidencing a nearly linear dependence of  $\log(T_{1/2}^\alpha)$  on the square root of  $Q_\alpha$ . There is a small curvature to the plots, but this occurs over many orders-of-magnitude. The systematic behavior is valuable for estimating the unmeasured half-life of a nuclide for which  $Q_\alpha$  is known. This is the initial basis for a prediction of the  $\alpha$  decay half-life of  $^{178}\text{Hf}^{m2}$ . Geiger-Nuttall systematics, however, reflect well-allowed decays and do not account for structure or angular momentum hindrances. In  $\alpha$  decay of  $^{178}\text{Hf}^{m2}$ , the high-spin of the initial state should strongly influence  $T_{1/2}^\alpha$ .

Hindrance factors in  $\alpha$  decay of odd-mass nuclei were discussed in Ref. [7], being given by the ratio of the measured

$T_{1/2}$  to an expected magnitude based on known values for  $\alpha$  transitions without spin change, typically in neighboring even-even nuclei. This approach combines hindrances arising due to different physical reasons. However, in principle, one may distinguish “macroscopic” and “spectroscopic” hindrances. The first hindrance arises in the case of particle emission with non-zero orbital momentum due to the centrifugal barrier. The second one reflects a structure hindrance due to the re-arrangement of single-particle orbits and of the nuclear spin orientation.

For electromagnetic decay, structure hindrances are typically isolated in reference to the standard decay rate theoretically predicted for transitions of known energy and multipolarity. In deformed nuclei such “ $K$  hindrances” were determined successfully for many transitions and the reduced hindrance factors were systematized. The latter parameter describes, in definition, the retardation factor reduced to one unit of the  $(\Delta K - \lambda)$  value, where  $\lambda$  is a multipolarity of the transition.

Here we extend this scheme to  $\alpha$  decay. The  $\alpha$  decay of  $^{178}\text{Hf}^{m2}$  seems ideal for this development, having strong changes of both spin and  $K$  in  $\alpha$  transitions to the yrast band of  $^{174}\text{Yb}$ . Such transitions are selected as they possess the highest  $Q_\alpha$  values (see Figs. 1 and 2). We first use the empirical systematics of Fig. 2 to estimate  $\alpha$  decay half-lives without hindrances, next construct a systematic description for the spin hindrance from the centrifugal barrier, and then compare the “predicted” half-life with the measured one to determine the  $K$  hindrance.

A centrifugal barrier arises for any  $\alpha$  transition with spin change. For isolation of a corresponding retardation factor, consider experimental data on  $\alpha$  decay when the  $K$  quantum number makes no effect. Recall that  $K$  is defined as the projection of the angular momentum vector  $I$  on the symmetry axis. It does not exist in near-magic spherical nuclei or in nuclei with nonaxial shapes. For evaluation of the spin-hindrance, we assume that  $K$  does not exist and the  $\alpha$  decay rate for transitions between initial  $I_i$  and final  $I_f$  states may be expressed as

$$R = \frac{N_{at} \ln 2}{T_{1/2}^\alpha (Q_\alpha^{if})} \sum_{m=-I_f}^{I_f} \frac{1}{F(|I_i - m|)}, \quad (1)$$

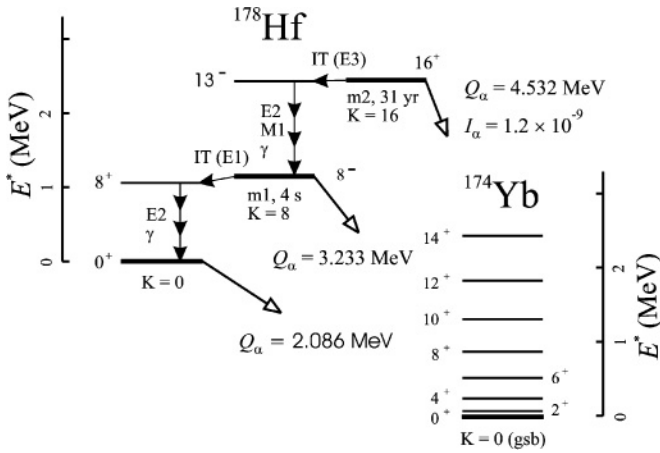


FIG. 1.  $\alpha$  decay scheme for  $^{178}\text{Hf}$  nuclei in the ground and isomeric states. The  $Q_\alpha$  values were deduced from the nuclear mass tables [4] and the level energies and angular momenta from Ref. [5]. The presently measured absolute intensity is given for  $\alpha$  decay of the  $m2$  level to be  $1.2 \times 10^{-9}$ .

where  $Q_\alpha^{if}$  is the transition energy,  $m$  is the projection of  $\vec{I}_f$  along the direction of  $\vec{I}_i$ ,  $N_{at}$  is the number of decaying nuclei and  $T_{1/2}^\alpha(Q_\alpha^{if})$  corresponds to a value from Fig. 2 that depends only on  $Q_\alpha^{if}$  and assumes zero spin change. The  $F(|I_i - m|) = F(\ell)$  is defined as the spin-hindrance factor and depends only on the difference in spins between initial and final states. If  $I_i = 0$ , the sum in Eq. (1) may be replaced by the spin volume factor  $(2I_f + 1)$  divided by  $F(I_f)$ .

Data exists in the literature on the relative intensities for branches of  $\alpha$  decay for ground states of even-even nuclei that reach levels in the ground-state band of the daughter nuclide. The initial and final states are characterized by  $K = 0$  so it

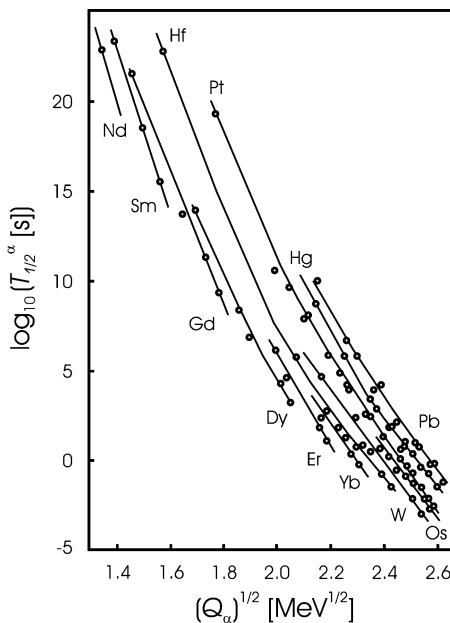


FIG. 2. Geiger-Nuttall systematics of  $\alpha$  decay half-lives for nuclei in the range of  $Z = 60-82$ .

was possible to isolate the spin-hindrance factor at  $\Delta I = I_f$ . Data [5] for  $^{230}\text{Th}$  and  $^{238}\text{Pu}$  were analyzed using Eq. (1) and the corresponding Geiger-Nuttall curves. With this procedure, values of the spin hindrance function  $F(\ell)$  were characterized up to  $\ell = 8$ .

For  $\alpha$  decay of  $^{178}\text{Hf}^{m2}$ , the spin difference could be as high as  $\Delta I = 16$ , so the  $F(\ell)$  values extracted from Th and Pu are insufficient. To extend  $F(\ell)$  to higher spin differences, data were used for  $\alpha$  decay of the high-spin isomers  $^{211m}\text{Po}$  ( $25/2^+$ ),  $^{212m}\text{Po}$  ( $18^+$ ) and  $^{214m2}\text{Rn}$  ( $8^+$ ). These nuclei demonstrate pure manifestation of spin hindrance in  $\alpha$  decay. They are near-magic nuclei so their  $\alpha$  decays proceed without structure retardation.

For each of these nuclei, a ratio was taken between the isomer's half-life for  $\alpha$  decay giving a specific  $\Delta I$  and the ground state's  $\alpha$  decay half-life for a specific  $\Delta I$ . This ratio of half-lives was then related to the difference between the spin changes caused by the isomer and ground-state  $\alpha$  decays to determine  $F(\ell)$ . The difference between spin changes was not so large for  $^{211}\text{Po}$ : even though a branch of the isomer's  $\alpha$  decay provides as much as  $\Delta I = 12$ , the ground state  $\alpha$  decay causes  $\Delta I = 4$ . However, for  $^{212}\text{Po}$  and  $^{214}\text{Rn}$  the spin difference is equal to the spin released in the isomer decay. In this manner, Eq. (1) was used to obtain  $F(\ell)$  up to  $\ell = 18$  and confirming the  $\ell \leq 8$  values.

Figure 3 shows the extracted  $F(\ell)$  function. The magnitude of this hindrance is very high for  $\ell$  up to 16, of importance for the estimation of  $\alpha$  decay of the  $I^\pi = 16^{+178}\text{Hf}^{m2}$  isomer. By analogy with electromagnetic decay, one can introduce a reduced hindrance factor  $f$  for  $\alpha$  decay according to  $F(\ell) = f^\ell$ , also given in Fig. 3; despite the scatter the trend suggests a choice of  $f = 6.8$  for high  $\ell$  numbers. Thus, the necessary components are now available to obtain a reliable

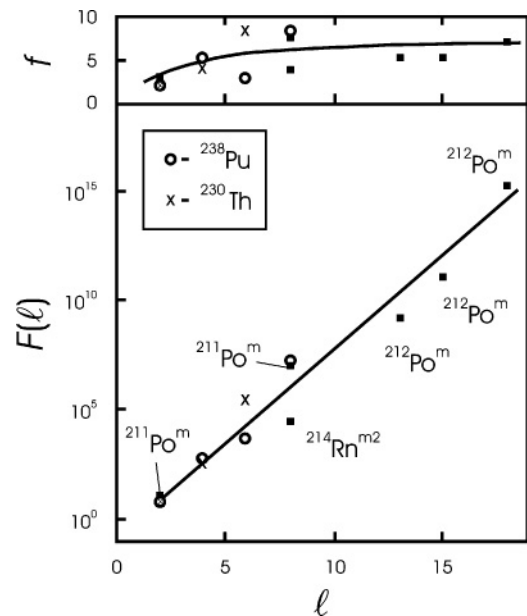


FIG. 3. Spin hindrance  $F(\ell)$  versus angular momentum taken by the emitted  $\alpha$  particle (bottom panel) and the reduced hindrance  $f$  (top panel). Three points marked as  $^{212m}\text{Po}$  correspond to different branches of its  $\alpha$  decay.

TABLE I. Estimated partial half-lives for  $\alpha$  decay of the  $^{178}\text{Hf}^{m2}$  isomer to levels in the ground-state band of  $^{174}\text{Yb}$ . The calculations are discussed in the text.

Transition $I_i \rightarrow I_f$	$E_\alpha$ [MeV]	$T_{1/2}^{\alpha,f}$ [yr]
$16^+ \rightarrow 0^+$	4.43	$8.6 \times 10^{10}$
$16^+ \rightarrow 2^+$	4.35	$3.0 \times 10^9$
$16^+ \rightarrow 4^+$	4.18	$3.4 \times 10^8$
$16^+ \rightarrow 6^+$	3.91	$1.2 \times 10^8$
$16^+ \rightarrow 8^+$	3.56	$2.8 \times 10^8$
$16^+ \rightarrow 10^+$	3.12	$2.7 \times 10^9$
$16^+ \rightarrow 12^+$	2.61	$7.2 \times 10^{10}$
$16^+ \rightarrow 14^+$	2.03	$5.5 \times 10^{13}$

estimate of the  $\alpha$  decay half-life of  $^{178}\text{Hf}^{m2}$  based on empirical information.

The partial  $\alpha$  decay half-lives,  $T_{1/2}^{\alpha,f}$ , are given in Table I for the transitions from the  $I_i^\pi = 16^+ \text{ } ^{178}\text{Hf}$  isomeric state to levels in the ground-state band of  $^{174}\text{Yb}$  with  $I_f^\pi = 0^+ - 14^+$ . The values in the table were obtained using Eq. (1) where the dominant contribution in the summation corresponds to the minimum  $\Delta I$ . This occurs because  $F(\ell)$  is a very steep function. The shortest half-life is expected for decay that reaches the  $6^+$  level of the daughter, giving the optimum product of  $T_{1/2}^{\alpha,f}(Q_\alpha^{i,f})$  and  $F(\ell)$ . Using the partial half-lives, the total  $\alpha$  decay half-life is estimated to be  $T_{1/2}^\alpha = 6.4 \times 10^7$  y. The  $\alpha$  decay represents a low-intensity branch compared to electromagnetic decay of the isomer, thus requiring a sensitive measurement.

A source of  $^{178}\text{Hf}^{m2}$  containing about  $3.5 \times 10^{13}$  atoms with isomeric nuclei was prepared about ten years ago [8] at the Flerov Laboratory of Nuclear Reactions, JINR. The hafnium fraction was chemically isolated from the enriched  $^{176}\text{Yb}$  target after exposing it to a 36-MeV  $^4\text{He}$ -ion beam. The hafnium fraction containing  $^{178}\text{Hf}^{m2}$  activity was deposited onto a Be foil and formed a hafnium oxide layer; no hafnium carrier was used in the chemical preparation. The thickness of the layer was small, definitely allowing small energy losses for transmission of  $\alpha$  particles. The only hafnium in the material was that produced by nuclear reactions within the high-purity and highly-enriched  $^{176}\text{Yb}$  target. The purity of the hafnium material was guaranteed by several methods [8], including neutron activation analysis.

A first measurement was performed using a Si surface barrier (SSB) detector with active area of 14-mm diameter. The  $^{178}\text{Hf}^{m2}$  source was placed in vacuum at 10 mm from the SSB detector. The absolute efficiency of the detector was calibrated using a  $^{\text{nat}}\text{U}$  sample and the energy resolution was found to be better than 50 keV. The  $^{178}\text{Hf}^{m2}$  source was kept for two weeks in the chamber, pumped twice per week by a dry system. A spectrum of  $\alpha$  particles was collected and a background spectrum was also measured during a two-week period under identical conditions, but without a source.

Single events were observed in both spectra. An  $\alpha$  energy range from 2.0–4.5 MeV was selected so as to cover all branches listed in the table. The total number of events within the selected range was obtained for the “effect” spectrum (with

source) and the “background” spectrum (without source). Subtracting the “background” number from the “effect” value gave  $N_\alpha = (-17 \pm 25)$  as the number of  $\alpha$  decays from the  $^{178}\text{Hf}^{m2}$  source during the two-week period. Correcting to the detector efficiency, one obtains an upper limit for  $\alpha$  emission from the source at  $\leq 1$  alpha per 3 hours. This gives  $T_{1/2}^\alpha > 6.6 \times 10^9$  y for  $^{178}\text{Hf}^{m2}$  and a  $K$ -hindrance factor  $> 100$ .

No statistically-significant emission, above background, was detected within the entire range of energies from 2 to 9 MeV. The background level must be attributed to contamination of the vacuum chamber, etc., which were composed of regular technical materials like stainless steel. It was decided to employ a more sensitive detection method rather than to attempt an improvement of sensitivity with SSBs by increasing the acquisition time, installing multiple detectors or preparing a more purified vacuum chamber.

Low-background charged-particle detection has been known for decades using solid-state track detectors. This approach is well-developed and has been calibrated by many groups, including at JINR (see Refs. [9,10]). In the present experiment for  $\alpha$  detection, CR-39 foils were used as produced by “Track Analysis Systems Ltd, UK.” These detector-quality foils were produced from very pure materials and contain no  $\alpha$  active contaminants. Thus, in measurements with these foils the only source of background could be by penetration of radon. The track detector foil is provided with a clean polyethylene film cover to exclude radon. The film is removed prior to use. During experiments, the foils must remain isolated from the surrounding air. Thus, the  $^{178}\text{Hf}^{m2}$  source was pressed between two clean CR-39 foils and carefully wrapped by plastic. The sandwich was then sealed for months within a plastic box since plastic materials contain less contamination from U and Th than metal packing.

Tracks due to  $\alpha$  particles appeared in the exposed detector foil after etching the foil to develop those tracks. The tracks were counted by visual registration using an optical microscope. The foil facing the source had an  $\alpha$  detection integral efficiency of about 80% from  $2\pi$ , according to previous calibrations. The rear-positioned foil was useful to determine the background.

After seven-months exposure to the source, the surfaces of the exposed CR-39 detector foils showed moderate damage. A rough spot was present on the foil past etching, seen directly by the naked eye in the region where the active material was placed. This diffuse damage was interpreted as being caused by a high flux of low-energy electrons emitted from the source. Tracks of  $\alpha$  particles were nevertheless discerned and counted, but it was decided to reduce the electron-induced damage to the foil surface.

Additional series were carried out in which detector foils were exposed to the hafnium source for shorter periods of 1 and 3.5 months. The etching time was slightly shortened as well to minimize the development of the diffuse damage spot. Under these conditions the degree of damage on the surface of the detector foil due to electrons was significantly reduced. Tracks of  $\alpha$  particles were observed clearly and in accordance with their standard configuration. The total number of tracks within the area in contact with the active spot of the source

was integrated and was consistent with the number found in the first experiment with CR-39 when normalized for time. The region in the facing foils away from the source, without exposure to  $\alpha$  particles, was also examined to determine the level of background.

Complementary background measurements were performed with similar CR-39 foils kept in the same environment and placed in contact with various non- $\alpha$  active foils including a Be foil similar to that which served as substrate for the hafnium source. The background was also measured without any material in contact with a detector. In all cases, the background track densities were statistically identical and also identical to the value obtained from the detector foil used with the hafnium sample (facing the sample), but away from the active spot.

The background track number was measured with good statistical accuracy to be 160 events and was then used to define the excess of counts due to the presence of the  $^{178}\text{Hf}^{m2}$  activity. The three exposure runs covered a total duration of about one year and the results were integrated to deduce 307 excess counts due to  $\alpha$  activity of the source, giving  $2.1\alpha/\text{day}$  after time and efficiency correction. During the measurement period, the number of  $^{178}\text{Hf}^{m2}$  nuclei was about  $2.8 \times 10^{13}$ , so that

$$T_{1/2}^{\alpha} = (2.5 \pm 0.5) \times 10^{10} \text{ y}. \quad (2)$$

This significantly improves the estimate of Ref. [11] of  $T_{1/2}^{\alpha} > 6 \times 10^8 \text{ y}$  for  $^{178}\text{Hf}^{m2}$ . The present measurement error exceeds a 10% statistical error since systematic errors

could not be excluded, for instance, due to the uncertainty in the efficiency of detection. Spectral information on  $^{178}\text{Hf}^{m2}$   $\alpha$  decay is based only on the theoretical values given in the table as the experiments did not allow groups to be distinguished in the  $\alpha$  spectrum.

The measured  $T_{1/2}^{\alpha}$  is larger than the estimated value by a factor of 390. One can interpret this as a manifestation of  $K$  hindrance in  $\alpha$  decay. A  $K$  hindrance of only  $4 \times 10^2$  is quite low for  $\alpha$  decay of  $^{178}\text{Hf}^{m2}$ . For example, one of the dominant decay branches seen in the table reaches the  $6^+$  level in  $^{174}\text{Yb}$  via a transition with degree of  $K$  forbiddenness  $\nu = (\Delta K - \Delta I) = 6$ . In comparison, the corresponding spin hindrance  $F(\ell = 6) \sim 10^5$  is seen in Fig. 3. This suggests that in reality  $K$  hindrance is weakly manifested in  $\alpha$  decay of  $^{178}\text{Hf}^{m2}$  and the  $K$  quantum number plays a relatively small role.

A theoretical analysis of  $\alpha$  decay half-lives is given in Refs. [12,13]. For the ground state of  $^{178}\text{Hf}$ ,  $T_{1/2}^{\alpha} \sim 5 \times 10^{23} \text{ y}$  was found [12]. The measured value for the  $^{178}\text{Hf}^{m2}$  isomer is much shorter,  $T_{1/2}^{\alpha} = 2.5 \times 10^{10} \text{ y}$ . This is the sustained manifestation of the gain in  $Q_{\alpha}$  value due to the 2.446-MeV excitation energy of the isomer as shown in Fig. 1. The retardation of  $\alpha$  decay by angular momentum creates a factor of many orders-of-magnitude and, after accounting for this effect, a relatively weak  $K$  hindrance was deduced from the experimental  $T_{1/2}^{\alpha}$  value.

This work was supported by Youngstown State University as part of Battelle contract TCN04177 from the U.S. Army Research Laboratory (contract DAAD19-02-D-0001).

- 
- [1] M. B. Smith, P. M. Walker, G. C. Ball *et al.*, Phys. Rev. C **68**, 031302(R) (2003).  
 [2] S. M. Mullins, G. Dracoulis, A. P. Byrne *et al.*, Phys. Lett. **B393**, 279 (1997); **B400**, 401 (1997).  
 [3] A. Aprahamian, R. C. de Haan, H. G. Börner *et al.*, Phys. Rev. C **65**, 031301(R) (2002).  
 [4] P. Möller, J. R. Nix, W. D. Myers, and W. J. Swiatecki, At. Data Nucl. Data Tables **59**, 185 (1995).  
 [5] R. B. Firestone and V. S. Shirley, *Table of Isotopes*, 8th ed. (Wiley, New York, 1996).  
 [6] H. Geiger and J. M. Nuttall, Phil. Mag. **22**, 613 (1911).  
 [7] M. R. Schmorak, Nucl. Data Sheets **31**, 283 (1980).  
 [8] Yu. T. Oganessian, S. A. Karamian, Yu. P. Gangrsky *et al.*, in *Proceedings of the International School-Seminar "Heavy-Ion Physics,"* Dubna, Russia, (JINR, Dubna, 1993), Vol. I, p. 365.  
 [9] S. P. Tretyakova, Yu. S. Zamiatnin, V. N. Kovantsev *et al.*, Z. Phys. A **333**, 349 (1989).  
 [10] S. A. Karamian, F. Grüner, W. Assmann *et al.*, Nucl. Instrum. Methods B **193**, 144 (2002).  
 [11] J. van Klinken, W. Z. Venema, R. V. F. Janssens *et al.*, Nucl. Phys. A **339**, 189 (1980).  
 [12] C. Xu and Z. Ren, Phys. Rev. C **69**, 024614 (2004).  
 [13] V. Yu. Denisov and H. Ikezoe, Phys. Rev. C **72**, 064613 (2005).